MUK PUBLICATIONS
Open Access Publisher

International Jr, of Qualitative Theory of Differential Equations and Applications
Vol. 2 No. 2 (December, 2016)
ISSN: 0973-3590

A mathematical model for sickle cell depolymerization: dynamical properties and numerical experiments

Nikki Daniel-Jones[a], Mingxiang Chen[b]*,
Dominic P. Clemence[b], Gregory Gibson[b]

[a] *PO Box 1214 Greensboro, NC 27402*
[b] *Department of Mathematics, North Carolina A&T State University, Greensboro, NC 27411*

Abstract. This paper considers a mathematical model to assess the effects of carbon monoxide (CO) on sickle cell hemoglobin (HbS) during HbS polymer melting. Assuming a buffer solution in which a mixture of HbS solution and fibers is rapidly mixed with CO, the model describes the subsequent dynamic interaction of four phases of the HbS components. Stability analysis of the model is presented in the CO-free case, the CO-saturated case and the general case. Numerical experiments are reported which monitor the effects of CO levels in the buffer solution. The model supports the proposition that CO binds directly to solution phase as well as polymerized HbS, and it predicts that while all the HbS becomes CO-bound at equilibrium, not all the HbS fibers are necessarily melted, indicating the presence of CO-bound fiber molecules.

AMS Subject Classifications: 34A34, 34K20, 37C70, 92D25, 92D30, 92C45

Keywords: Sickle cell depolymerization; HbS-CO binding; Sickle cell mathematical models; System of nonlinear differential equations; Asymptotic behaviors

1. Introduction

Sickle cell disease is an inherited genetic blood disorder that affects red blood cells. The disease is due to the mutation of the sixth position of the beta globin chain of hemoglobin, where the amino acid glutamic acid (which is hydrophilic) of normal

E-mail addresses: ndjones04@yahoo.com (N. Daniel-Jones), chen@ncat.edu (M. Chen), clemence@ncat.edu (D. Clemence), gagibson@ncat.edu (G. Gibson)
*Corresponding author

hemoglobin (HbA) is replaced with the amino acid valine (which is hydrophobic) to become sickle cell hemoglobin (HbS). The mutated HbS may become hard, sticky and shaped like sickles due to lack of oxygen. When these hard and pointed red cells go through the small blood vessels, vascular occlusion may occur, causing pain, tissue damage and low blood count (anemia) complications which constitute sickle cell disease. The disease occurs most commonly in Africa, the Mediterranean, and India; about eight percent of African-Americans have sickle cell trait–carrying the sickle cell gene but not showing the disease.

Sickle cell pathogenesis is known to be driven by a polymerization-depolymerization cycle which coincides with the circulation cycle of blood of about 15 seconds fueled by the re-oxygenation in the lungs. Sickle hemoglobin exists as isolated units in the red cells when oxygenated. But when the deformed HbS release oxygen to the peripheral tissues, they tend to stick together and form long chains (polymers). The HbS polymers are held together by very weak forces, and when the red cells return to the lungs and pick up oxygen again, the hemoglobin molecules resume their solitary existence. HbS molecules, which have a life of about sixteen days, undergo repeated processes of polymerization and depolymerization. While the mechanism for polymerization is well-described as double nucleations by Ferrone et al [7], [8], the mechanism for depolymerization is not at all known [1], and its characterization is of interest in the design of sickle cell relief therapies. The purpose of this paper is to describe and analyze a mathematical model that considers how carbon monoxide (CO) affects HbS during HbS polymer melting, and to use the model to understand the mechanism for the HbS fiber melting process.

The authors in [2] have considered the effect of CO on HbS during fiber melting, and they have proposed a model in the form of a system of linear equations to compare with their experimental data. Their model was based on the assumptions that fibers only melt from the ends, and that CO can only bind to solution phase HbS. The present paper will describe a nonlinear model that extends the original two-species model of [8] to a four-species one which incorporates CO-binding to polymerized HbS. Theoretical models for ligand-induced melting of HbS fibers are desirable as inexpensive tools for the preliminary study and evaluation of the effects of ligands such as CO on HbS fiber melting.

The rest of this article is organized as follows. In the next section, the original model formulated in [8] and the extension in [2] are recalled, and an extended model is described. Results on the dynamics of the extended model are presented in Section 3 together with their proofs and a discussion about their biological significance. Numerical experiments on CO effects are described and discussed in Section 4, with a concluding discussion in Section 5.

2. The Mathematical Model

2.1. The preliminary Models

We first recall the basic models proposed in [8] and [2]. The fundamental observation in [8] is that the growth of HbS fibers is described by the equation

$$-\frac{dC_m(t)}{dt} = (k_+ C_m(t) - k_-)C_p(t) \tag{2.1}$$

(equation (3), [8] page 614) where $C_p(t)$ and $C_m(t)$ are the respective molar concentrations of the polymerized and solution-phase HbS, while k_+ and k_- are the respective rate constants for polymerization and melting in a given solution buffer. Here, we understand that the term $-\frac{dC_m(t)}{dt}$ is the rate of disappearance of monomers, the term $k_+C_m(t)C_p(t)$ is due to monomers associating to heterogeneous nucleus (existing polymers) and the term $-k_-C_p(t)$ is due to dissociation of monomers from polymers.

In [2], based on the hypothesis that polymer melting only occurs at the polymer ends, the authors made the assumption that the number of polymers would be constant. They then used C_p to denote the constant number of polymers and replaced the $C_p(t)$ in (2.1) by C_p, they let the equilibrium relation $k_+ = \frac{k_-}{C_s}$ (where C_s is the solubility concentration of the buffer) and let $k^d = k_-$ indicate the de-oxygenated (de-oxy) melting rate constant, so that the equation (2.1) was rewritten as

$$\frac{dC_m(t)}{dt} = -k^d(\frac{C_m(t)}{C_s} - 1)C_p. \tag{2.2}$$

Letting $C_p^*(t)$ (note: we changed the original notation $C_p'(t)$ used in [2] and [3] to avoid possible confusion with derivative notation) be the concentration of hemoglobin in polymer phase, and with the assumption that the total HbS molar concentration would be constant, that is $C_p^*(t) + C_m(t) = C_{tot}$ =constant, equation (2.2) leads to

$$\frac{dC_p^*(t)}{dt} = k^d(\frac{C_m(t)}{C_s} - 1)C_p. \tag{2.3}$$

To investigate the effect of CO binding to sickle cell polymers during melting, the authors in [2] made a differentiation of the solution phase population $C_m(t)$ into two sub-populations: $C_m^{co}(t)$, the molecules which are CO-bound, and $C_m^d(t)$, those which are not CO-bound (or de-oxy). Under the assumption that CO can only bind to solution phase hemoglobin molecules, the rate of change of $C_m^{co}(t)$ only comes from the binding of CO to $C_m^d(t)$. This leads to the following three-equation model proposed in [2] to monitor the experimentally observed concentration of de-oxy HbS molecules

in experiments incorporating CO-mediation:

$$\frac{dC_m^d(t)}{dt} = -k^d(\frac{C_m^d(t)}{C_s^{1.53}} - 1)C_p - k_m[CO]C_m^d(t) \tag{2.4}$$

$$\frac{dC_m^{CO}(t)}{dt} = k_m[CO]C_m^d(t) \tag{2.5}$$

$$\frac{dC_p^*(t)}{dt} = k^d(\frac{C_m^d(t)}{C_s^{1.53}} - 1)C_p \tag{2.6}$$

where the following nomenclature is used:

$C_m^d(t)$: Molar concentration of deoxy HbS in the solution phase
$C_p^*(t)$: Molar concentration of deoxy HbS cells in the polymer phase
$C_m^{co}(t)$: Molar concentration of CO-bound HbS in the solution phase
C_p: Molar concentration of HbS polymer fibers
[CO]: Molar concentration of carbon monoxide
k_m: CO binding (ligation) rate for solution phase HbS
k^d: Dissociation (melting) rate constant of de-oxy HbS cells
$C_s^{1.53}$: Solubility concentration of 1.53M phosphate buffer

Notice that system (2.4)-(2.5)-(2.6) is linear and can be solved in the following order: first solve (2.4) for $C_m^d(t)$ (because C_p is a constant), then solve (2.5) for $C_m^{co}(t)$ and (2.6) for $C_p^*(t)$. However, the experimental data did not fit the dynamics of the solution ([2]) and the authors rejected the model as unsuitable.

2.2. The Extended Model

To extend the model (2.4)-(2.5)-(2.6), we first rescind the assumption that 'the concentration of polymers in the HbS sample remains constant during melting.' As in [8], we use $C_p(t)$ and $C_m(t)$ to represent molar concentrations of the polymerized HbS and solution-phase HbS respectively, and set $C_p(t) + C_m(t)$ =constant. From the kinetic equation (2.1), we thus obtain the following modification of (2.2) and (2.3):

$$\frac{dC_m(t)}{dt} = -k^d(\frac{C_m(t)}{C_s} - 1)C_p(t) \tag{2.7}$$

$$\frac{dC_p(t)}{dt} = k^d(\frac{C_m(t)}{C_s} - 1)C_p(t). \tag{2.8}$$

Next, we incorporate CO-mediation as in [2], but we rescind the assumption that 'CO can only bind to solution phase hemoglobin molecules'. This allows us to differentiate the polymerized population $C_p(t)$ into two sub-populations: $C_p^{co}(t)$, which are CO-bound, and $C_p^d(t)$, which are not CO-bound, or de-oxy. This is in addition to the differentiation of $C_m(t)$ into two sub-population $C_m^{co}(t)$ and $C_m^d(t)$. These considerations result in the segregation of HbS cells into the following class compartments for the HbS cells during polymer melting:

	De-oxy	CO-bound
Polymers	C_p^d	C_p^{co}
Monomers	C_m^d	C_m^{co}

Now, the assumed CO-binding results in a loss from the class of de-oxy HbS in solution phase $C_m^d(t)$, which translates into a gain for the CO-bound solution phase HbS $C_m^{co}(t)$, with a CO-mediated binding rate constant k_m. Similarly, the assumed CO-binding to polymer phase molecules, with CO-mediated binding rate constant k_p results in a loss from the $C_p^d(t)$ class, which effects a gain to the $C_p^{co}(t)$ class. Finally, the loss of these polymer phase molecules, with CO-mediated dissociation rate constant k^{co} leads to a gain for the $C_m^{co}(t)$ population.

To derive the equations involving the CO-free HbS components, we first let $C_m(t)$ in (2.7)-(2.8) be replaced by $C_m^d(t)$ and $C_p(t)$ by $C_p^d(t)$. The CO-binding to the population $C_m^d(t)$ results in a loss to $C_m^d(t)$, and the CO-binding to the population $C_p^d(t)$ results in a loss from $C_p^d(t)$, so we add the term $-k_m[CO]C_m^d(t)$ to the right hand side of (2.7), and $-k_p[CO]C_p^d(t)$ to the right hand side of (2.8). These result in

$$\frac{dC_m^d(t)}{dt} = -k^d(\frac{C_m^d(t)}{C_s} - 1)C_p^d(t) - k_m[CO]C_m^d(t) \tag{2.9}$$

and

$$\frac{dC_p^d(t)}{dt} = k^d(\frac{C_m^d(t)}{C_s} - 1)C_p^d(t) - k_p[CO]C_p^d(t)) \tag{2.10}$$

Similarly, To derive the equations involving the CO-bound HbS components, we let $C_m(t)$ in (2.7)-(2.8) be replaced by $C_m^{CO}(t)$ and $C_p(t)$ by $C_p^{CO}(t)$. Note that the loss from $C_m^d(t)$ is a gain for $C_m^{co}(t)$, and the loss from $C_p^d(t)$ is a gain for $C_p^{co}(t)$, so we add the term $k_m[CO]C_m^d(t)$ to the right hand side of (2.7) and add $k_p[CO]C_p^d(t)$ to the right hand side of (2.8). These result in

$$\frac{dC_m^{co}(t)}{dt} = k^{co}(1 - \frac{C_m^d(t)}{C_s^{co}})C_p^{co}(t) + k_m[CO]C_m^d(t) \tag{2.11}$$

and

$$\frac{dC_p^{co}(t)}{dt} = -k^{co}(1 - \frac{C_m^d(t)}{C_s^{co}})C_p^{co}(t) + k_p[CO]C_p^d(t) \tag{2.12}$$

The model (2.9)-(2.10)-(2.11)-(2.12) allows CO-binding to polymers, and that melting may occur at the endpoints as well as the surfaces of polymer fibers. It is a slight variant of the model described in [3] where the $C_p^d(t)$ term in (2.9) and (2.10) is C_p^*, and the term $\frac{C_m^d(t)}{C_s^{co}}$ in (2.11) and (2.12) is absent.

3. Dynamical Properties of the Model

In this section, we analyze the extended sickle cell model to obtain the dynamical properties. Before proceeding, we re-order (2.9)-(2.10)-(2.11)-(2.12) into (2.9)-(2.11)-(2.10)-(2.12), and simplify notation by replacing $(C_m^d(t), C_m^{co}(t), C_p^d(t), C_p^{co}(t))$ by (x, y, z, u), and $(k^d, k_m[CO], k^{co}, k_p[CO], C_s, C_s^{co})$ by $(k_1, k_2, k_3, k_4, C_1, C_2)$ to write the system as follows:

$$\frac{dx}{dt} = -k_1(\frac{x}{C_1} - 1)z - k_2 x \tag{3.1}$$

$$\frac{dy}{dt} = k_3(1 - \frac{y}{C_2})u + k_2 x \tag{3.2}$$

$$\frac{dz}{dt} = -k_4 z + k_1(\frac{x}{C_1} - 1)z \tag{3.3}$$

$$\frac{du}{dt} = -k_3(1 - \frac{y}{C_2})u + k_4 z. \tag{3.4}$$

3.1. Main Results

The main dynamical results of the model are stated below.

In the CO-free case ($[CO] = 0$), there is no CO-mediated melting ($k^{co} = 0$), and thus, $k_2 = 0$, $k_3 = 0$ and $k_4 = 0$, so that the system (3.1)-(3.4) becomes

$$\frac{dx}{dt} = -k_1(\frac{x}{C_1} - 1)z \tag{3.5}$$

$$\frac{dz}{dt} = k_1(\frac{x}{C_1} - 1)z \tag{3.6}$$

and its dynamical behavior is summarized in the following results:

Theorem 3.1. *(CO-free case) Let $x_0 \geq 0$, $z_0 \geq 0$, $x_0 + z_0 = c$ and $x(t, x_0, z_0)$, $z(t, x_0, z_0)$ be the solution of (3.5)-(3.6) with $x(0) = x_0$, $z(0) = z_0$.*

(i) If $z_0 = 0$ then $x(t, x_0, 0) = x_0 = c$ and $z(t, x_0, 0) = 0$ for all $t \geq 0$.

(ii) Assume $c \leq C_1$. If $0 \leq x_0 < c$ and $z_0 > 0$, then $x(t, x_0, z_0)$ is increasing on $[0, \infty)$ and $\lim_{t\to\infty} x(t, x_0, z_0) = c$, $z(t, x_0, z_0)$ is decreasing on $[0, \infty)$ and $\lim_{t\to\infty} z(t, x_0, z_0) = 0$.

(iii) Assume $c > C_1$. If $x_0 = C_1$, $z_0 = c - C_1$ then $x(t, x_0, z_0) = x_0$ and $z(t, x_0, z_0) = z_0$ for all $t \geq 0$; if $x_0 \neq C_1$ and $z_0 > 0$, then $x(t, x_0, z_0) \to C_1$ monotonically and $z(t, x_0, z_0) \to c - C_1$ monotonically.

In the CO-saturated case, $x(t) = 0$ and $z(t) = 0$, and the system (3.1)-(3.4) is reduced to

$$\frac{dy}{dt} = k_3(1 - \frac{y}{C_2})u \tag{3.7}$$

$$\frac{du}{dt} = -k_3(1 - \frac{y}{C_2})u. \tag{3.8}$$

The dynamical behaviors are described as follows:

Theorem 3.2. *(CO-saturated case) Let $y_0 \geq 0$, $u_0 \geq 0$, $y_0 + u_0 = c$, and $y(t, y_0, u_0)$, $u(t, y_0, u_0)$ be the solution of system (3.7)-(3.8) with initial condition $y(0) = y_0$, $u(0) = u_0$.*

(i) If $u_0 = 0$ then $y(t, y_0, 0) = y_0 = c$ and $u(t, y_0, 0) = 0$ for all $t \geq 0$.

(ii) Assume $c \leq C_2$. If $0 \leq y_0 < c$ and $u_0 > 0$, then $y(t, y_0, u_0)$ is increasing on $[0, \infty)$ and $\lim_{t\to\infty} y(t, y_0, u_0) = c$, $u(t, y_0, u_0)$ is decreasing on $[0, \infty)$ and $\lim_{t\to\infty} u(t, y_0, u_0) = 0$.

(iii) Assume $c > C_2$. If $y_0 = C_2$, $u_0 = c - C_2$ then $y(t, y_0, u_0) = y_0$ and $u(t, y_0, u_0) = u_0$ for all $t \geq 0$; if $y_0 \neq C_2$ and $u_0 > 0$, then $y(t, y_0, u_0) \to C_2$ monotonically and $u(t, y_0, u_0) \to c - C_2$ monotonically.

For the general system (3.1)-(3.4), we have the following:

Theorem 3.3. *(general case) Let $x_0 \geq 0$, $y_0 \geq 0$, $z_0 \geq 0$, $u_0 \geq 0$, $x_0 + y_0 + z_0 + u_0 = c$, and $x(t, x_0, y_0, u_0)$, $y(t, x_0, y_0, u_0)$, $z(t, x_0, y_0, u_0)$, $u(t, x_0, y_0, z_0, u_0)$ be the solution of system (3.1)-(3.4) with $x(0) = x_0$, $y(0) = y_0$, $z(0) = z_0$, $u(0) = u_0$.*

(i) The solution preserves nonnegativity, i.e., $x(t) \geq 0$, $y(t) \geq 0$, $z(t) \geq 0$ and $u(t) \geq 0$ for all $t \geq 0$ if $x(0) \geq 0$, $y(0) \geq 0$, $z(0) \geq 0$ and $u(0) \geq 0$.

(ii) For any initial data x_0, y_0, u_0, $z(t, x_0, y_0, 0, u_0) = 0$, $x(t, 0, y_0, 0, u_0) = 0$, $u(t, x_0, y_0, 0, 0) = 0$ and $y(t, 0, 0, 0, 0) = 0$ for all $t \geq 0$.

(iii) If $c \leq C_2$, then the solution $(x(t), y(t), z(t), u(t)) \to (0, c, 0, 0)$ as $t \to \infty$.

(iv) If $c > C_2$, then the solution $(x(t), y(t), z(t), u(t)) \to (0, C_2, 0, c - C_2)$ as $t \to \infty$.

3.2. Proofs of Main Results

The proofs of the above theorems are given below.

Proof of Theorem 3.1. Note that the system (3.5)-(3.6) implies that $\frac{dx}{dt} + \frac{dz}{dt} = 0$, and therefore $x + z = x_0 + z_0 = c$, a constant; if we substitute $z = c - x$ into (3.5), we then obtain a scalar equation,

$$\frac{dx}{dt} = -k_1(\frac{x}{C_1} - 1)(c - x). \tag{3.9}$$

Equation (3.9) has two equilibria: $x = C_1$ and $x = c$. Let $x(t, x_0)$ be the solution of (3.9) with $x(0) = x_0$. Analyzing the phase portrait for cases $c < C_1$, $c = C_1$ and $c > C_1$, it is easy to see that: if $c \leq C_1$, then $x(t, c) = c$ for all $t \geq 0$; the solution $x(t, x_0)$ with $x_0 < c$ is increasing and it approaches c as $t \to \infty$ (Figures 1a and 1b); if $c > C_1$, then $x(t, c) = c$, and the $x(t, x_0)$ with $x_0 \neq C_1$ and $x_0 < c$ approaches C_1 monotonically as $t \to \infty$ (see Figure 1c). Using the fact that $z(t) = c - x(t)$, Theorem 1 is proved.

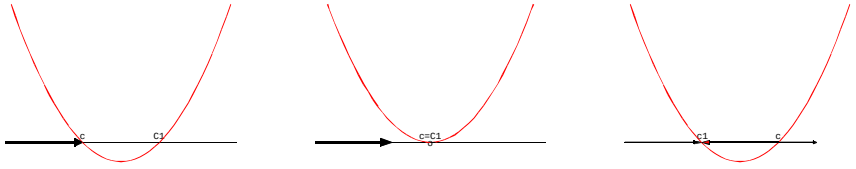

(1a) $c < C_1$ (1b) $c = C_1$ (1c) $c > C_1$

Figure 1: Phase line portrait of $\frac{dx}{dt} = -k_1(\frac{x}{C_1} - 1)(c - x)$

Proof of Theorem 3.2. The proof is very similar to that of Theorem 3.1, and we omit it.

For the proof of Theorem 3.3, we first present two lemmas to simplify discussion.

Lemma 3.1. *Let function $w(t)$ be continuously differentiable on interval $I = [0, \tau)$, $0 < \tau \leq \infty$. Assume that $w(0) \geq 0$ and $w'(t_1) > 0$ whenever $w(t_1) = 0$, $t_1 \in I$; then $w(t) > 0$ on $(0, \tau)$.*

Proof. Assume the conclusion were not true. If $w(0) > 0$, then there is a $t_1 > 0$ such that $w(t) > 0$ on $[0, t_1)$ and $w(t_1) = 0$, which imply that $w'(t_1) \leq 0$. But by the given condition we should have $w'(t_1) > 0$ since $w(t_1) = 0$; thus there is a contradiction, and we must have $w(t) > 0$ on the whole interval $[0, \tau)$. If $w(0) = 0$ then $w'(0) > 0$; and thus $w(t) > 0$ at least in some open interval $(0, a)$. A similar argument shows that we must have $w(t) > 0$ for all $t \in (0, \tau)$.

Lemma 3.2. *Consider the system*

$$\frac{dx}{dt} = -k_1(\frac{x}{C_1} - 1)z - k_2 x, \tag{3.10}$$

$$\frac{dz}{dt} = -k_4 z + k_1(\frac{x}{C_1} - 1)z. \tag{3.11}$$

with $k_1 > 0$, $k_2 > 0$, $k_4 > 0$, and $C_1 > 0$. If $x_0 \geq 0$ and $z_0 > 0$, then $x(t) > 0$, $z(t) > 0$ for all $t > 0$, and $x(t) \to 0$, $z(t) \to 0$ exponentially. If $z_0 = 0$ and $x_0 \geq 0$, then $z(t) = 0$ and $x(t) \geq 0$ for all $t \geq 0$, and $x(t) \to 0$ exponentially.

Proof. Let

$$a(t) = -[\frac{k_1 x(t)}{C_1} + k_2] \quad \text{and} \quad b(t) = -k_4 + k_1[\frac{x(t)}{C_1} - 1]$$

then the system (3.10)-(3.11) can be written as

$$\frac{dx}{dt} = a(t)x + k_1 z, \qquad \frac{dz}{dt} = b(t)z.$$

It follows that

$$z(t) = z_0 e^{\int_0^t b(s)ds}, \qquad x(t) = e^{\int_0^t a(s)ds}[x_0 + k_1 \int_0^t e^{-\int_0^s a(\tau)d\tau} z(s)ds].$$

The expressions immediately yield that $z(t) > 0$ and $x(t) > 0$ for $t > 0$ on the interval of existence if $z_0 > 0$ and $x_0 \geq 0$. Moreover, letting $k = \min\{k_1, k_4\}$ one has

$$\frac{d(x+z)}{dt} = -k_2 x - k_4 z \leq -k(x+z).$$

Hence

$$0 \leq x(t) + z(t) \leq (x_0 + y_0)e^{-kt}$$

for $t > 0$ and on the interval of existence, thus $x(t)$ and $z(t)$ are bounded and the interval of existence is $[0, \infty)$, further, both $x(t)$ and $z(t)$ converge to 0 exponentially as $t \to \infty$. It is easy to see that $z_0 = 0$ implies that $z(t) = 0$ for all $t \geq 0$. The Lemma is proved.

Proof of Theorem 3.3. We now consider the complete system (3.1)-(3.4). Note that $x(t) + y(t) + z(t) + u(t) = c$.

Part (ii) is easy to check.

For the proof of parts (i), (iii) and (iv), using the facts that (3.1) and (3.3) are unrelated to y and u, and that $x(t) \geq 0$, $z(t) \geq 0$ for all $t \geq 0$ and $x(t) \to 0$ and $z(t) \to 0$ by Lemma 3.2, we only need to show the non-negativity and boundedness of $y(t)$ and $u(t)$, then discuss the asymptotic behavior of $y(t)$ and $u(t)$.

We consider the following three cases.

Case 1: $x_0 = 0$ and $z_0 = 0$. Then $x(t) = 0$ and $z(t) = 0$ for all $t \geq 0$, and the original system is reduced to a system with two equations as in the CO-saturated case discussed in Theorem 3.2. So $y(t)$ and $u(t)$ are nonnegative and bounded, $y(t) \geq 0$ and $u(t) \geq 0$, $y(t) \to c$ and $u(t) \to 0$ if $c \leq C_2$; $y(t) \to C_2$ and $u(t) \to c - C_2$ if $c > C_2$. Parts (i), (iii) and (iv) are therefore true in this case.

Case 2: $x_0 \geq 0$ and $z_0 > 0$. Then by Lemma 3.2, $x(t) > 0$ for all $t > 0$ and $z(t) > 0$ for all $t \geq 0$. We claim that $u(t) > 0$ for all $t > 0$. If not, suppose there is a $t_1 \geq 0$ such that $u(t_1) = 0$. However, using (3.4) we have $\frac{du}{dt}(t_1) = k_4 z(t_1) > 0$, so $u(t) > 0$ for all $t > 0$ and t in the interval of existence of $u(t)$ by Lemma 3.1. We also claim that $y(t) > 0$ for all $t \geq 0$. If not, then there is a $t_2 \geq 0$ such that $y(t_2) = 0$. If $t_2 > 0$, then $\frac{dy}{dt}(t_2) = k_3 u(t_2) + k_2 x(t_2) > 0$ by (3.2), and again by Lemma 1, we must

have $y(t) > 0$ for all $t > 0$ and t in the interval of existence of $y(t)$. If $t_2 = 0$ (that is, $y_0 = 0$), then as long as $u_0 \neq 0$ or $x_0 \neq 0$, we still have $\frac{dy}{dt}(0) = k_3u_0 + k_2x_0 > 0$, therefore $y(t) > 0$ for all $t > 0$ and and t in the interval of existence by Lemma 3.1. If $y_0 = 0$ with both $x_0 = 0$ and $u_0 = 0$, then $\frac{dy}{dt}(0) = 0$ and we cannot use Lemma 3.1. However, as $z_0 > 0$ and

$$\frac{d^2y}{dt^2}(0) = k_3\frac{du}{dt}(0) + k_2\frac{dx}{dt}(0) = k_3k_4z_0 + k_2k_1z_0 > 0$$

(by differentiating (3.2) and using $x_0 = y_0 = u_0 = 0$), then $\frac{d^2y}{dt^2}(t) > 0$ on $[0, \tau_1)$ with some $\tau_1 > 0$. Using the Taylor expansion of $y(t)$ at 0, $y(t) = \frac{1}{2}y''(s)t^2 > 0$, where $0 < s < t$, for all $t \in (0, \tau_1)$; then from the above discussion, we have $y(t) > 0$ for all $t > 0$ and t in the interval of existence. Part (i) is therefore true in this case.

Case 3: $x_0 > 0$ and $z_0 = 0$. Then $z(t) = 0$ for all $t \geq 0$ and $x(t) = x_0e^{-(\frac{k_1}{C_1}+k_2)t} \to 0^+$ monotonically. We claim that if $y_0 \geq 0$ and $u_0 > 0$, then $y(t) > 0$ and $u(t) > 0$ for all $t > 0$; and if $y_0 \geq 0$ and $u_0 = 0$, then $y(t) > 0$ and $u(t) = 0$ for all $t > 0$. In fact, as $z(t) = 0$, then $\frac{du}{dt} = -k_3(1 - \frac{y}{C_2})u$ by (3.4) and so $u(t) = u_0e^{-\int_0^t k_3(1-\frac{y}{C_2})d\tau} \geq 0$ as long as $y(t)$ and $u(t)$ exist. We show that $y(t) > 0$ on its interval of existence. In fact, if there is a $t_1 \geq 0$ with $y(t_1) = 0$, then $\frac{dy}{dt}(t_1) = k_3u(t_1) + Kcx(t_1) > 0$ by (3.2), so that $y(t) > 0$ by Lemma 3.1. Part (i) is thus also true in this case.

We have shown in Case 2 and Case 3 that all $x(t), y(t), z(t)$ and $u(t)$ are nonnegative. As the sum $x(t) + y(t) + z(t) + u(t) = c$ is a positive constant, $y(t)$ and $u(t)$ are nonnegative and bounded, and thus they exist on $[0, \infty)$.

Next, We discuss the asymptotic behavior of $y(t)$ and $u(t)$. Using boundedness and the Bolzano-Weierstrass theorem, there is a subsequence $t_k \to \infty$ with $y(t_k) \to y_1$, $u(t_k) \to u_1$ and $y_1 + u_1 = c$ since $x(t) \to 0$, $z(t) \to 0$ as $t \to \infty$. By the theory of dynamical systems (see [9]), for any nontrivial and nonnegative initial data (x_0, y_0, z_0, u_0), the $\omega-$limit set $\omega(x_0, y_0, z_0, u_0)$ is nonempty, compact, invariant, and attracts. Moreover,

$$\omega(x_0, y_0, z_0, u_0) \subset L = \{(0, y, 0, u) | y \geq 0, u \geq 0, y + u = c\}$$

and

$$\omega(x_0, y_0, z_0, u_0) \subset \omega(L).$$

But the discussion of the CO-saturated case (Theorem 3.2) shows that for any initial point on L, we have $\omega(L) = (0, C_2, 0, c - C_2)$ if $c > C_2$, or $\omega(L) = (0, c, 0, 0)$ if $c \leq C_2$. Therefore, $\omega(x_0, y_0, z_0, u_0) = \omega(L)$ is a singleton. Part (iii) and (iv) are therefore proved.

3.3. Biological Significance of Main Results

Theorems 3.1-3.3 may be interpreted as having the following biological significance.

Theorem 3.1: In the CO-free case, there is no carbonated Hbs, and so $C_p^{co}(t) = 0$ and $C_m^{co}(t) = 0$.

(i) If there are no initial de-oxy polymers ($C_p^d(0) = 0$), then all de-oxy monomers stay as they are ($C_m^d(t)$ =constant); this is consistent with expectation as there are no polymers to melt.

(ii) If there are some initial de-oxy polymers ($C_p^d(0) > 0$), and if the total HbS population is no more than the solubility concentration of phosphate ($c \leq C_s$), then all de-oxy polymers will melt into de-oxy monomers ($C_p^d(t) \to 0$ and $C_m^d(t) \to c$).

(iii) If there are some initial de-oxy polymers ($C_p^d(0) > 0$), and if the total HbS population is more than the solubility concentration of phosphate ($c > C_s$) , then either the de-oxy polymers melt into de-oxy monomers when the initial monomer population is less than the solubility concentration of phosphate ($C_m^d(0) < C_s$) until the solubility concentration of phosphate is reached ($C_m^d(t)$ increases to C_s and $C_p^d(t)$ reduces to $c - C_s$); or there is de-oxy polymerization from de-oxy monomers when the initial monomer population is more than the solubility concentration of phosphate ($C_m^d(0) > C_s$) until the solubility concentration of phosphate is reached ($C_m^d(t)$ reduces to C_s and $C_p^d(t)$ increases to $c - C_s$).

Theorem 3.2: In the CO-saturated case (Theorem 3.2), there is no de-oxy Hbs, and so $C_p^d(t) = 0$ and $C_m^d(t) = 0$.

(i) If there are no initial CO-bound polymerized HbS ($C_p^{co}(0) = 0$), there is no polymer melting, and all CO-bound solution phase HbS stay as they are ($C_m^{co}(t)$ =constant);

(ii) If there are some initial CO-bound polymerized HbS ($C_p^{co}(0) > 0$), and if the total HbS population is no more than the CO-solubility concentration ($c \leq C_s^{co}$), then all CO-bound polymers will melt into CO-bound solution phase HbS ($C_p^{co}(t) \to 0$ and $C_m^{co}(t) \to c$);

(iii) If there are some initial CO-bound polymerized HbS ($C_p^{co}(0) > 0$), and if the total HbS population is more than the CO-solubility concentration ($c > C_s^{co}$), then either the CO-bound polymerized HbS melt into CO-bound solution phase HbS when the initial CO-bound solution phase HbS population is less than the carbon solubility concentration ($C_m^{co}(0) < C_s^{co}$) until the CO-solubility concentration is reached ($C_m^{co}(t)$ increases to C_s^{co} and $C_p^{co}(t)$ reduces to $c - C_s^{co}$); or there is CO-bound polymerization from CO-bound solution phase HbS when the initial CO-bound solution phase HbS population is more than the CO-solubility concentration ($C_m^{co}(0) > C_s^{co}$) until the CO-solubility concentration is reached ($C_m^{co}(t)$ reduces to C_s^{co} and $C_p^{co}(t)$ increases to $c - C_s^{co}$);

Theorem 3.3: In the general case, with both de-oxy and carbonation effects are present.

(i) The non-negativity shows the model is consistent with the expectation that the population of each group remains non-negative, and the total HbS population remains unchanged.

(ii) As there is CO ($[CO] > 0$) and CO-bound activity ($k_m > 0$ and $k_d > 0$), there are eventually no de-oxy HbS ($C_m^d(t) \to 0$ and $C_p^d(t) \to 0$)), that is, the HbS are either in CO-bound solution phase or in CO-bound polymerized phase.

(iii) If the total HbS population is no more than the CO-solubility concentration ($c \leq C_s^{co}$), then eventually all HbS are in CO-bound solution phase ($C_p^{co}(t) \to 0$ and $C_m^{co}(t) \to c$).

(iv) If the total HbS population is more than the CO-solubility concentration ($c > C_s^{co}$), then there are eventually only CO-bound solution phase HbS ($C_m^{co}(t) \to C_s^{co}$) and CO-bound polymerized HbS ($C_p^{co}(t) \to c - C_s^{co}$).

4. Numerical Experiments

4.1. The Experiments

In this section, we report numerical experiments which assess the effects of varying the levels of CO in the solution on the transient dynamics. The following parameter and initial values from [2] are used:

k_m	$= 0.070$	$\pm\ 0.002$	(s-1mM-1) Binding rate of CO to solution phase HbS
k^d	$= 0.028$	$\pm\ 0.0008$	(1/s) Melting rate for de-oxy HbS monomers
k_p	$= 0.010$		(s-1mM-1) Binding rate of CO to de-oxy HbS polymers
k^{CO}	$= 0.100$		(1/s) Melting rate of CO-bound HbS polymers
$C_s^{1.53}$	$= 0.4000$		(mM) Solubility concentration of phosphate buffer (dil)
C_s^{CO}	$= 0.1000$		(mM) Solubility concentration of CO

and

$C_m^d(0)$	$= 0.0036$ (mM)	Molar concentration of de-oxy HbS monomers
$C_m^{CO}(0)$	$= 0.0000$ (mM)	Molar concentration of CO-bound HbS monomers
$C_p^d(0)$	$= 0.1750$ (mM)	Molar concentration of de-oxy HbS polymers
$C_p^{CO}(0)$	$= 0.0000$ (mM)	Molar concentration of CO-bound HbS polymers

To observe the CO-effects, we kept all parameters and initial values constant and varied the molar concentration of CO $[CO]$, from 0.05 to 909.1. We used $C++$ to generate the numerical solutions and to plot the data to visualize the results. We have the following observations for the four HbS components.

The analysis in Section 3 (Theorem 3.3) shows that for $[CO] > 0$, $C_m^d(t)$ always goes to 0 as t increases; the decrease, however, this change is not always monotone, as we will now show. From equation (2.9), let

$$A = -k^d(\frac{C_m^d(0)}{C_s} - 1)C_p^d(0), \quad B = k_m[CO]C_m^d(0), \quad \text{and } M = \frac{dC_m^d(0)}{dt},$$

so that the slope of $C_m^d(0)$ is given by $M = A$ - $B[CO]$. Notice that $B > 0$ since all of our parameters are positive. If $C_m^d(0) < C_s$ then $A > 0$, and when $CO = 0$, $M = A > 0$. As $[CO]$ increases the slope decreases until it becomes 0 and then negative. The value of $[CO]$ for which the initial slope $M = 0$ is $[CO] = \frac{A}{B}$. For the initial conditions used here, $\frac{A}{B} = 19.269$. Figure 2 shows the effects of varying $[CO]$ on $C_m^d(t)$.

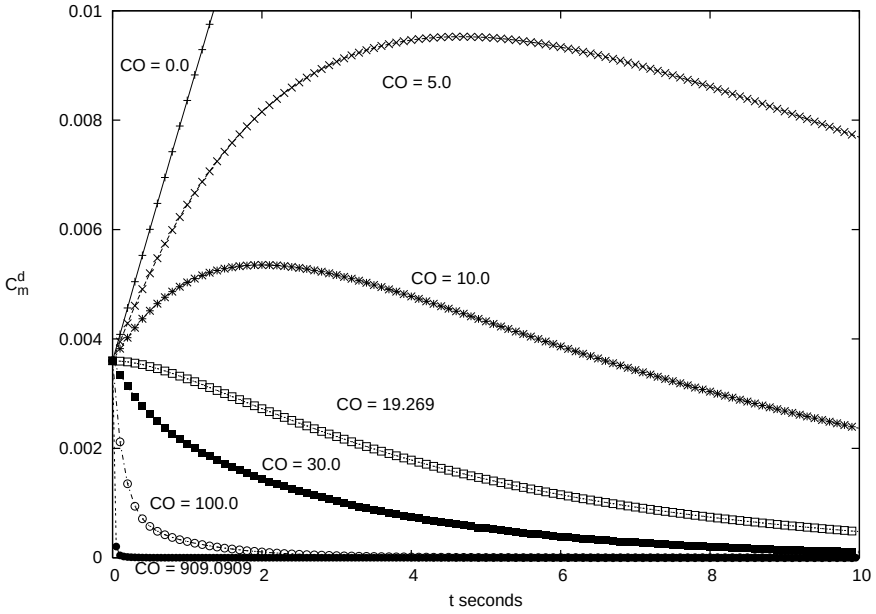

Figure 2: The effect of CO levels on C_m^d. Note the transition in qualitative behavior at $[CO] = 19.629$.

Equation (2.10) gives the rate of change for C_p^d. When $C_m^d < C_s$, the second term, $k^d(\frac{C_m^d(t)}{C_s} - 1)C_p^d(t)$, is negative, with the first term, $-k_p[CO]C_p^d(t)$, also negative since all parameters are positive, making the derivative $\frac{dC_p^d(t)}{dt}$ negative. As CO increases, the magnitude of the first term increases, making the derivative more negative. As it can be seen from Figure 3, this simply causes C_p^d to decrease more rapidly to 0, without altering the qualitative behavior.

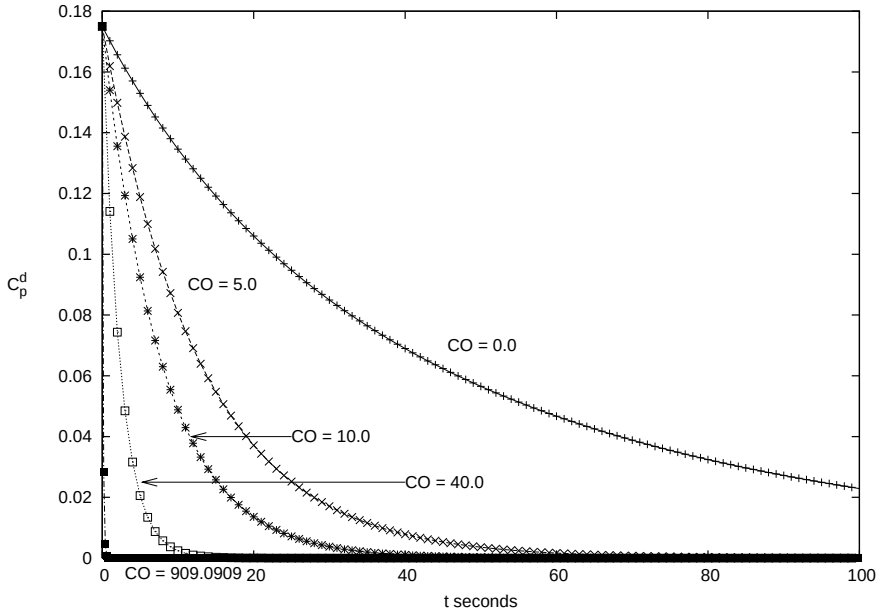

Figure 3: Effect of CO levels on C_p^d.

Like C_m^d, the component C_m^{co} is not monotonic for small values of CO. The numerically determined transition value for $C_m^d(t)$ with given parameters and initial conditions to change behavior appears to be approximately at $[CO] = 8.6$, as seen in Fig 4. That is, for $[CO] < 8.6$, C_m^{co} increases to a value above the equilibrium, then decreases to the equilibrium; for $[CO] > 8.6$, C_m^{co} increases monotonically to the equilibrium.

The component C_p^{co} displays some very interesting behavior as levels of CO vary. For large enough levels, with the stated initial conditions and parameter values, C_p^{CO} increases rapidly for a very short time and then decreases toward the equilibrium value, as seen in Fig 5. For very small $[CO]$ values C_p^{co} increases, decreases, then increases toward the equilibrium value. This behavior is shown in Fig 6.

4.2. Discussion of Numerical Experiments

Our numerical experiments reveal case (iv) in Theorem 3. The numerical results show that for large CO there is an initial rapid increase in C_p^{CO} followed by a decrease of C_p^{co} to the equilibrium $C_m^d(0) + C_m^{co}(0) + C_p^d(0) + C_p^{co}(0) - C_s^{co} = 0.0786$. This suggests a fast CO attachment to C_p^d (C_p^d transits to C_p^{co}) which is then followed by CO-aided melting, since the initial rapid increase in C_p^{co} (Fig 5) corresponds to an initial rapid decrease in C_p^d (Fig 3); and the following gentle decrease of C_p^{co} to equilibrium corresponds to a gentle increase of C_m^{CO} (Fig 4) to equilibrium $C_s^{co} = 0.1$, the slow

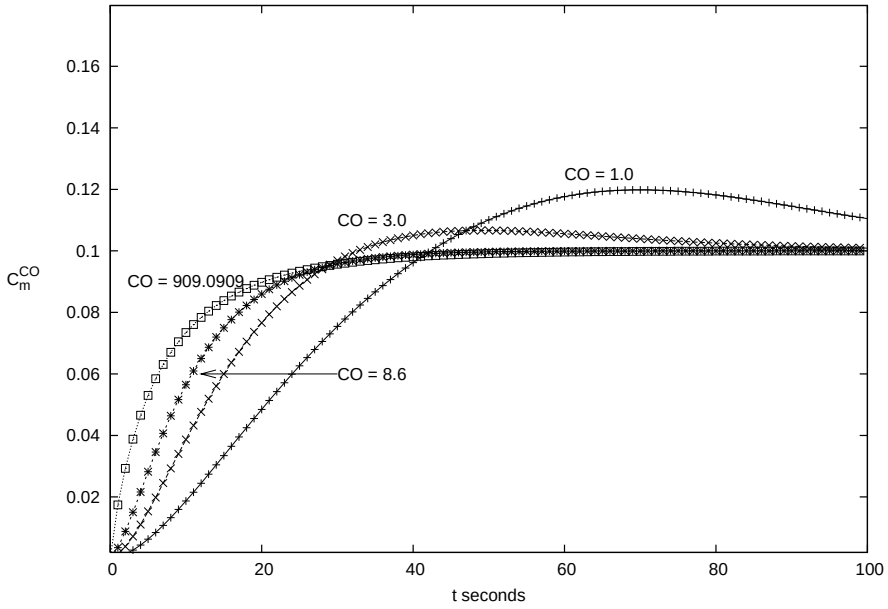

Figure 4: Effect of CO levels on C_m^{CO}, note the transition at $CO = 8.6$.

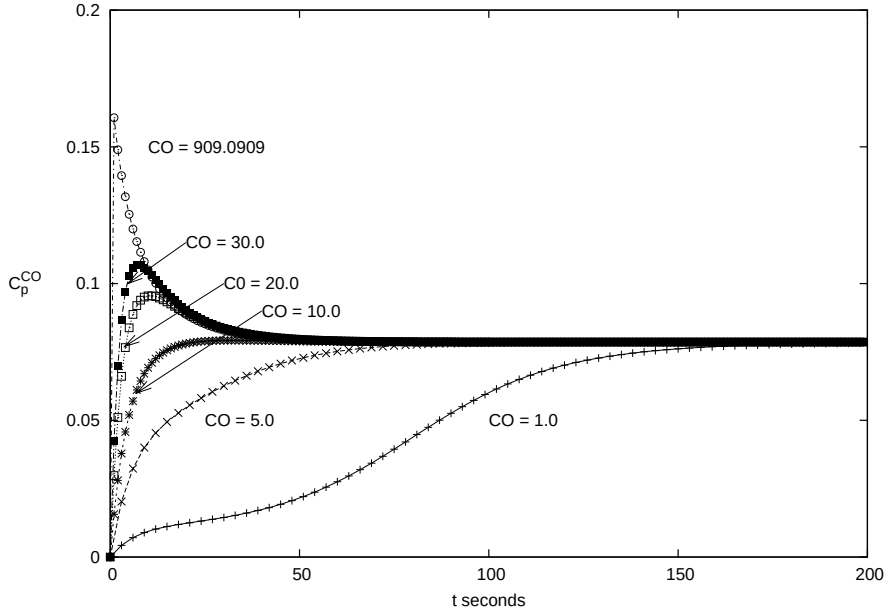

Figure 5: Effect of CO levels on C_p^{CO}.

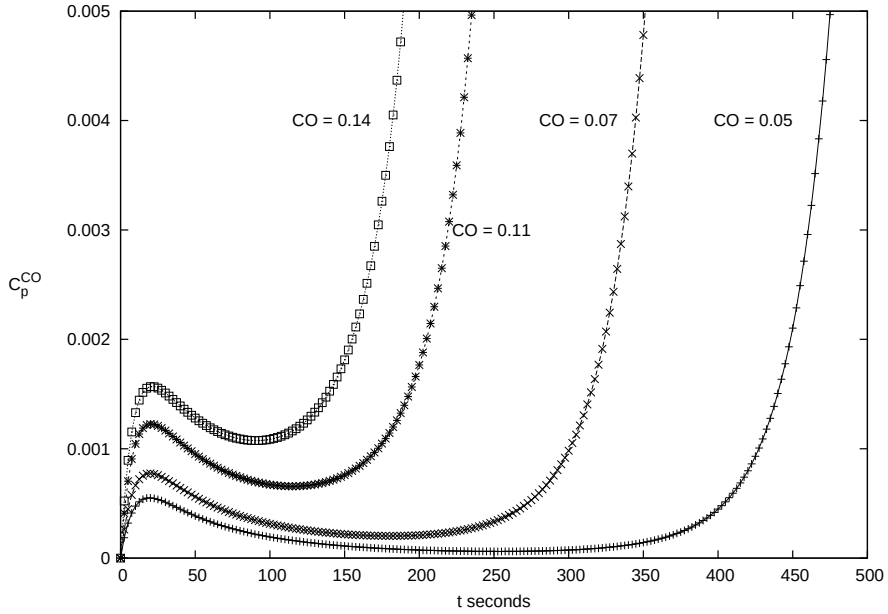

Figure 6: Effect of very small CO levels on C_p^{CO}.

decrease suggesting a relatively gentle melt of C_p^{CO}.

For CO $\leq$ 19.269, the initial increase in C_m^d is followed by a gentle decrease to equilibrium 0. This suggests that C_m^d increases due to non CO-aided melting of C_p^d in this regime, followed by the gentle loss of C_m^d due to CO attachment. In this regime, the initial increase in C_m^d and following decrease correspond to an initial decrease in C_p^d followed by an increase in C_m^{CO}, which suggests a melting of de-oxy polymers followed by CO-attachment to de-oxy monomers (HbS in solution phase) at low CO-concentrations.

We use the following diagram to illustrate the implications of our experiments. The numerical experiments suggest that the path 1-2 is dominant for low CO, while the path 3-4 is dominant for high CO.

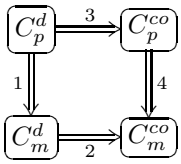

Moreover, for low CO, C_m^{CO} experiences a steep initial growth on a scale corresponding to an initial steep decay in C_m^d, suggesting fast initial attachment of CO to C_m^d. However, the simulation suggests that this CO attachment is unstable - CO-attached C_m^{CO} reverts back to de-oxy C_m^d or returns to C_p^{CO}. However, since $\frac{d}{dt}C_p^{co}(0) < 0$ for

low CO, it must be that C_m^{CO} turns into C_m^d, suggesting weak CO-attachment to C_m^d at low CO concentration.

5. Conclusion

A mathematical model for the dynamic behavior of a mixed population of free and polymerized HbS molecules in a CO-saturated buffer solution has been described and qualitatively analyzed. Numerical experiments were performed to study the effects of CO on melting dynamics of the polymers. The model further predicts that, at high enough CO-solubility concentrations, CO binds to all HbS, both solution phase HbS and and polymerized HbS, and all are CO-ligated before 0.5 seconds for the parameters and initial values used in [2]. However, while the de-oxy polymerized HbS population does disappear from the solution, the CO-ligated polymerized population exceeds the CO-ligated free population until almost 8 seconds, and complete melting does not occur until about 41 seconds. Based on the parameter values used in our simulations, our experiments confirm the conclusion reached in [2] that carbon binding during sickle cell polymer melting is possible, and does increase the melting rate of the polymers, resulting in a very short time interval during which melting occurs.

Acknowledgements The authors are grateful to Svetlana Aroutiounian for her suggestions and discussions about the model described in the paper. The authors would like to acknowledge the support from NASA grant No. NAG 9-1402, and a NC A&T State University 2006-2007 Futures grant.

The authors would like to thank the referees for suggestions on simplifyng the proof of Lemma 3.2 and valuable comments which have improved exposition.

References

[1] Gunjan Agarwal, Jiang Cheng Wang, Suzanna Kwong, Scott M. Cohen, Frank A. Ferrone, Robert Josephs4 and Robin W. Briehl, Sickle Hemoglobin Fibers: Mechanisms of Depolymerization, J. Mol. Biol. 322 (2002) 395-412.

[2] S. K. Aroutiounian, J. G. Louderback, S. K. Ballas, D. B. Kim-Shapiro, Evidence for carbon monoxide binding to sickle cell polymers during melting, Biophysical Chemistry, Volume 91, Number 2 (2001) 167-181.

[3] S. K. Aroutiounian, Seminar presentation in the Department of Mathematics, NC A & T State University, 2002, and Nikki Daniel-Jones, Undergraduate Honor's Report, 2004.

[4] R. W. Briehl, Nucleation, fiber growth and melting, and domain formation and structure in sickle cell hemoglobin gels, J. Mol. Biol. 245 (1995) 710-723.

[5] William A. Eaton and James Hofrichter, Sickle Cell Hemoglobin Polymerization, Advances in Protein Chemistry, Volume 40 (1990) 263-279.

[6] William A. Eaton, James Hofrichter and P. D. Ross, Delay time of gelation: a possible determinant of clinical severity in sickle cell disease, Blood, 4 (1976) 621-627.

[7] F. A. Ferrone, J. Hofrichter, and W. A. Eaton, Kinetics of sickle hemoglobin polymerization I. Studies using temperature-jump and laser photolysis techniques, J. Mol. Biol. 183 (1985) 591-610.

[8] F. A. Ferrone, J. Hofrichter, and W. A. Eaton, Kinetics of sickle hemoglobin polymerization. II. A double nucleation mechanism. J. Mol. Biol. 183 (1985) 611-631.

[9] Jack K. Hale, Asymptotic Behavior of Dissipative Systems, Mathematical Surveys and Monographs, Number 25, American Mathematical Society, Providence Rhode Island, USA, 1988.

[10] J. G. Louderback, S. K. Ballas and D. B. Kim-Shapiro, Sickle hemoglobin polymer melting in high concentration phosphate buffer, Biophys. J. 76 (1999) 2216-2222.

[11] A. Mozzarelli, J. Hofrichter and W. A. Eaton, Delay time of hemoglobin S polymerization prevents most cells from sickling in vivo, Science, 237 (1987) 500-506.

[12] D. B. Shapiro, R. M. Esquerra, R. A. Goldbeck, S. K. Ballas, N. Mohandas and D. S. Kliger, Carbon monoxide religation kinetics to sickle cell hemoglobin polymers following ligand photolysis, J. Biol. Chem. 270 (1995) 26078-26085.